Antifungal properties of nanosilver clay composites against fungal pathogens of agaricus bisporus.

ChemistrySelect

Research Article
doi.org/10.1002/slct.202301696

Chemistry Europe
European Chemical Societies Publishing

www.chemistryselect.org

Antifungal Properties of Nanosilver Clay Composites Against Fungal Pathogens of *Agaricus bisporus*

Tebogo Levy Ramakutoane,[a] Magaretha Petronella Roux-van der Merwe,[a] Jacqueline Badenhorst,[a] Sreejarani Kesavan Pillai,[b] and Suprakas Sinha Ray*[b, c]

This study aimed to determine the possible control of selected pathogenic and competitive fungi of *A. bisporus* by three nanosilver clay composites and establish the effective concentrations of the composites for inhibiting pathogens. Nanosilver (AgNPs) clay (zeolite, montmorillonite, and palygorskite) composites were synthesized by a microwave-assisted surface functionalization technique, and various techniques characterized the products. Zeolite and montmorillonite composites showed uniformly distributed spherical AgNPs with an average size of 3.33 nm and 2.85 nm, respectively, whereas palygorskite presented agglomerated and unevenly distributed AgNPs. The influence of the various composites on 9 fungi, including strains of *T. aggressivum* f. *aggressivum, L. fungicola, C. dendroides*, and *Mycogone* sp., was determined *in vitro* at different concentrations. At 10 mg/mL, AgNP-zeolite and AgNP-montmorillonite inhibited 8 out of 9 pathogens, while AgNP-palygorskite only inhibited 1 pathogen. The nanosilver clay composites tested against *A. bisporus* revealed no adverse effects on mycelial growth at any concentrations tested. This study confirms that AgNP-zeolite and AgNP-montmorillonite composites have effective antifungal properties and can be used as alternative fungicides against mushroom pathogens without affecting *A. bisporus* growth. However, further investigation is required to unravel the mechanism of selective antifungal activity observed in this study.

Introduction

Commercially, *Agaricus bisporus* is the most cultivated mushroom due to its substantial yields, desirable texture, and high nutritional value.[1] Mushroom cultivation and production can be hampered by the occurrence and development of various pests and pathogenic contaminants, such as viruses, bacteria, and fungi, which may negatively impact the yield and quality of mushrooms.[2,3] Among the contaminants that can occur in mushroom beds, mycopathogens are probably the most important, as these are fast-growing while competing with mushrooms for space and nutrients. These pathogens may also produce toxic secondary compounds, volatile organic compounds, and extracellular enzymes, which can cause decreased production or total crop loss.[3] Major fungal diseases of mushrooms include cobweb disease (caused by *Cladobotryum dendroides*), wet bubble disease (caused by *Mycogone perniciosa*), dry bubble disease (caused by *Lecanicillium fungicola*), and green mold disease (caused by *Trichoderma aggressivum* f. *aggressivum*).[4–10] Most mushroom growers employ various methods to control mycopathogens, including strict hygiene, steam sterilization, and chemical fungicide treatments.[1,11] Fungicides such as prochloraz-Mn, benomyl, chlorothalonil, thiabendazole, and carbendazim have been used in mushroom cultivation. Repeatedly using the same antifungal agents to control mycopathogens can result in resistant strains or strains with reduced sensitivity. Although prochloraz remains the most effective fungicide to control mushroom diseases, decreased sensitivity of *Lecanicillium* and *Cladobotryum* to this chemical has been recorded.[1,12,13] In addition, many chemicals lost approval for use in Europe, for example, chlorothalonil, carbendazim, and benzimidazoles, which have been banned or their use discouraged due to the adverse effects that they may have on the environment.[1,14] Due to these factors, alternative control measures have been sought to control mycopathogens in mushroom production. Biocontrol agents such as microorganisms (some *Bacillus* spp.), microbial by-products, and plant extracts (such as essential oils) have shown great promise as potential control agents due to their antifungal properties.[1,15–18] Currently, biocontrol agents have limited commercialization and control only a narrow range of mushroom pathogens.[19–22]

The use of silver nanoparticles (AgNPs) as antimicrobial agents has recently gained momentum. AgNPs have been known to possess both antibacterial and antifungal properties. The antimicrobial properties of AgNPs have been attributed to their high surface ratio and unique chemical and physical

[a] *T. L. Ramakutoane, Prof. M. P. Roux-van der Merwe, Prof. J. Badenhorst*
Department of Biotechnology and Food Technology, Tshwane University of Technology
175 Nelson Mandela Drive, Arcadia, Pretoria, 0083, South Africa

[b] *Dr. S. Kesavan Pillai, Prof. S. S. Ray*
Centre for Nanostructures and Advanced Materials
Council for Scientific and Industrial Research
1-Meiring Naude, Brummeria, Pretoria, 0184, South Africa
E-mail: rsuprakas@csir.co.za

[c] *Prof. S. S. Ray*
Department of Chemical Sciences
University of Johannesburg
Doornfontein, Johannesburg, 2028, South Africa
E-mail: ssinharay@uj.ac.za

properties that allow them to penetrate microbial cells.[23,24] Of the several methods to synthesize AgNPs, such as chemical, physical, and physicochemical, green chemistry methods have gained much more attention due to scalability, low cost, and eco-friendliness.[25,26] However, pure AgNPs tend to form agglomerates when synthesized. AgNPs synthesized on support materials, such as smectite clays, are smaller and distributed more uniformly.[27–29] Our research group reported a simple, faster, and environmentally friendly microwave-assisted synthesis method for immobilizing AgNPs on montmorillonite clay surfaces without reducing agents.[28] It has been shown that both the concentration and particle size of AgNPs influence antifungal efficacy[23,24,27] with an average particle size between 7–25 nm inhibiting *Fusarium oxysporum, Pythium spinosum*, and *Botrytis cinerea*, and the highest inhibition observed at 0.01 mg/mL.[30–32] In other studies, AgNPs of smaller sizes (3, 5, 8, and 10 nm) and different concentrations (0.0125–0.100 mg/mL) used against *Fusarium oxysporum* f. sp. *radicis-lycopersici* (FORL) strains,[31] showed improved activity with a decrease in particle size and increase in concentration. Although the antifungal potential of AgNPs has been established in some studies, these particles or their composites have (to the best of our knowledge) not been tested for their efficacy against mushroom fungal pathogens.

This study, therefore, aimed to determine the possible control of selected pathogenic and competitive fungi of *A. bisporus* by three nanosilver clay composites, as well as to determine the effect of nanosilver clay composites on *A. bisporus* mycelial growth. AgNP-containing clay composites were synthesized by functionalizing the surface of clays (zeolite, montmorillonite, and palygorskite) using a microwave-assisted heating technique, and various instrumental techniques characterized the composites. The influence of the composites and corresponding unmodified clays was determined on 9 fungi, including strains of *T. aggressivum* f. *aggressivum*, *L. fungicola, C. dendroides*, and *Mycogone* sp. at different concentrations (1-10 mg/mL) to establish the effective concentration of composites required for inhibition of pathogens while having no adverse effect on *A. bisporus.*

Experimental Section

Synthesis of Nanosilver Clay Composites

The characteristics of various nanoclays used in this research are summarized in Table 1. Microwave (MW) assisted synthesis of nanosilver clay composites was conducted by mixing approximately 10 g of nanoclay (zeolite/montmorillonite/palygorskite, mined at Heidelberg, plot 1412, Western Cape, South Africa, Ecca Holdings,

Table 1. Characteristics of zeolite, montmorillonite and palygorskite.

	Zeolite	Montmorillonite	Palygorskite
Chemical analysis (%) TYPICAL			
SiO_2	61.29	62.4	70.9
Al_2O_3	12.9	18.5	14.1
Fe_2O_3	2.36	3.3	5.3
TiO_2	0.16	0.2	0
CaO	1.35	1.2	1.6
MgO	1.61	4	5.7
K_2O	2.45	0.7	1.3
Na_2O	2.07	2.1	0.2
L.O.I.	15.76	7.5	0.9
Mineralogy (approximate)			
% Montmorillonite		80	
% Quartz	5	12	
% Clinopitile	90	1	
% Mica		7	
Physical properties			
Colour (Crude)	White - Grey	Cream-Pink	Off white
Appearance	Powder ($<$150microns)	Powder	Powder
Moisture (%)	$<$15	$\leq$15	6
Specific gravity (g/cm^3)	2.51	2.51	2.1
Loose bulk density (g/cm^3)	1.2	1.2	1.6
pH	8–9	9–11	6.5
Water absorption (on sinter plate)	400%	$\geq$ 450%	111%
Cation exchange capacity (meq/100 g)	20	$\geq$ 50	

South Africa) and 1000 mL of 0.1 M $AgNO_3$ (Sigma-Aldrich, Johannesburg, South Africa) into a typical synthesis batch and placing the mix in an Ultraclave high throughput microwave system (Milestone SCI, USA). The Ultraclave was operated at 2.45 GHz and a power setting of 900 W at 50 °C for 30 min (optimized conditions). Following the reaction, the mixture was filtered and washed with de-ionized water to remove excess silver (Ag^+) and (NO_3^-) ions. The residue was then dried at 50 °C overnight in an Eco-digitalTech oven (Labotec, Johannesburg, South Africa), ground into a powder using a pestle and mortar, followed by sieving to 75 μm.[28]

Characterization of Nanosilver Clay Composites

The possible formation of NPs from each prepared nanosilver clay composite sample was investigated using a JEOL 2100 TEM (Jeol Ltd., Tokyo, Japan), operated at 200 kV. Nanosilver clay composite samples were prepared for TEM analysis as follows; a small quantity of each nanosilver clay composite sample powder was individually sonicated in 1 mL of 95% methanol for 5 min.[28,30] The sample solutions were deposited on Cu-grids with holey carbon film (Sigma-Aldrich, Johannesburg, South Africa). Particle size distribution analysis was done on the TEM images (*circa* 200 particles) using ImageJ software (National Institute of Health, Maryland, USA). Elemental and silver loading analyses were performed using a NORAN EDS system (Thermo ScientificTM, Waltham, USA) attached to the JEOL 2100 TEM (Jeol Ltd., Tokyo, Japan). Infrared spectra of the pristine and nanosilver clay composites were obtained using an attenuated total reflectance Fourier-transform infrared (ATR FTIR) spectrometer (Perkin Elmer Spectrum 100 FTIR spectrometer, USA) from 4000 to 600 cm^{-1} through 16 scans at 4 cm^{-1}resolution.

Preparation of Spore Suspensions of Pathogenic Fungi

Fungi, obtained from the Pennsylvania State University (USA), namely *T. aggressivum* f. *aggressivum* (3 strains), *L. fungicola* (3 strains), *C. dendroides* (2 strains) and *Mycogone* sp. (1 strain) were grown on sterile malt extract agar (MEA) plates (Sigma-Aldrich, Johannesburg, SA), supplemented with (4 g/L) yeast extract (YE) (Sigma-Aldrich, Johannesburg, SA). The inoculated plates were incubated at 25 ± 2 °C until sporulation. After incubation, the fungal spores were washed from the mycelia using 10 mL of a sterile solution containing 0.05 g malt extract (ME) and 500 μL Tween 20 in 100 mL dH_2O (Sigma-Aldrich, Johannesburg, SA).[31] This solution, containing the fungal spores, was filtered through sterilized cheesecloth into an additional 90 mL of the sterile solution to remove any mycelial matter that may have accidentally been washed from the culture into the spore suspension. The spore suspensions were standardized to 1×10^5 spores/mL using a Neubauer haemacytometer (Smartlabs, Gauteng, South Africa).

Effect of Concentrations of Nanosilver Clay Composites on the Growth of Pathogenic Fungi

The antifungal properties of nanosilver clay composites were determined by preparing MEA plates supplemented with 4 g/L YE, as well as the individual nanosilver clay composites at 1–10 mg/mL concentration range (concentrations lower than 1 mg/mL were ineffective). A volume of 2 μL of the standardized spore (1×10^5 spores/mL) suspensions of the individual fungi was inoculated onto the center of MEA-YE plates containing a specific concentration of one of the nanosilver clay composites.[34] Fungi inoculated on MEA-YE plates without nanoclays and in the presence of respective unmodified clays were used as controls. All plates were incubated at 25 ± 2 °C for six days, and the mycelial growth of each fungus was measured using a digital caliper (KTV, Major Tech Pty Ltd, Isando, SA) on the 2^{nd}, 4^{th}, and 6^{th} day.

Effect of Nanosilver Clay Composites on the Growth of A. bisporus *in vitro*

For the cultivation of *A. bisporus*, a supplemented MEA-YE medium was prepared, containing MEA (50 g/L) and YE (4 g/L) dissolved in a water extract. This extract was prepared by heating a mixture of peat (30 g/L) and mushroom mycelium mix (70 g/L) to 100 °C for 5 min, followed by filtration. This medium was used to prepare six-well plates (Sigma-Aldrich, Johannesburg, SA) containing the three nanosilver clay composites (AgNP-zeolite, AgNP-montmorillonite, and AgNP-palygorskite) at 1 mg/mL, 5 mg/mL, and 10 mg/mL, respectively.[34] Control plates (supplemented MEA-YE), lacking AgNP composites, were also included. A single rye grain, colonized with *A. bisporus* mycelia (Sylvan Africa, Pretoria, SA), was placed at the center of each well. The plates were closed with microplate lids and incubated at 25 ± 2 °C for 14 days. The mycelial growth was measured throughout the incubation period, using a digital caliper (KTV, Major Tech Pty Ltd, Isando, SA).

Effect of AgNP-Zeolite, Applied Curatively, on the Fungal Pathogens *in vitro.*

The effect of AgNP-zeolite, applied as a solution, on actively growing mushroom pathogens was investigated by preparing MEA-YE in six-well plates (3 wells per pathogen). The fungal pathogens were inoculated by pipetting 2 μL of the standardized spore suspension (fungal pathogens) onto the middle of the plate. The plates were incubated at 25 ± 2 °C for 1 day for the *Trichoderma* spp. (fast-growing species) and 2 days for the other fungal pathogens, and the growth was measured using a digital caliper (KTV, Major Tech Pty Ltd, Isando, SA). After the measurements, 10 mg/mL of AgNP-zeolite was added to three of the six wells (assigned to a specific pathogen). In contrast, the other three wells were left to control untreated growth (no AgNP-zeolite solution was added).[33] The microplates were incubated at 25 ± 2 °C, and growth was measured, using a digital caliper, on the 2^{nd} and 3^{rd} days for *Trichoderma* spp. and the 4^{th} and 6^{th} days for the other fungal pathogens. The Effect of AgNP-zeolite on the morphology of mushroom pathogens was evaluated by a scanning electron microscope (SEM) (Carl Zeiss NTS GmbH, Oberkochen, Germany). The sample preparation was done according to the method of Hayat.[35]

Effect of AgNP-Zeolite on the Growth and Mushroom Production of *A. bisporus in vivo*

Mushroom beds (10 beds) were prepared by adding a 1.5 kg spawn mix (Highveld Mushrooms, Centurion, South Africa) to growing beds (length: 200 mm; height: 290 mm and width: 200 mm) and compacting it lightly. Additional spawn mix (50 g) and 700 g peat (Highveld Mushrooms, Centurion, South Africa) were mixed thoroughly with 10 mg/mL AgNP-zeolite and layered on the spawn mix.[34] Sampling ports were cut into the sides of the containers (mushroom beds). These openings were covered with masking tape to prevent liquid leakage during watering. Thermometers were inserted through the top of the beds (to the middle) to monitor the temperatures of the beds. The mushroom beds were placed in an incubation room, kept at 22 ± 2 °C and a humidity of 100%. Mushroom bed temperatures were kept at 26 ± 2 °C. Plastic sheeting was used to cover the surface of the mushroom beds to maintain high carbon dioxide concentrations during the spawning period. Distilled water was added to the mushroom beds in the volume of 370 mL and 740 mL on the 1st and 2nd day, while on the 3rd, 4th, and 5th day, the volume added was 1 L. After the watering cycle, samples (bed material) were obtained from the peat, top, and lower spawn layers. The samples were weighed and dried overnight in an Eco-digitalTech oven (Labotec, Johannesburg, South Africa) at 80 °C. The dried samples were ground into a powder (using a mortar and pestle) and sent to WaterLab (Pty) Ltd (Pretoria, South Africa) for ICP analysis to determine the silver concentration in the different layers of the mushroom beds.

From the 6th day until the end of cultivation, watering was only done after mushroom harvesting, between flushes. On the 8th day, the plastic sheeting was removed to release carbon dioxide. The room temperature was reduced by 1 °C per day until it reached 17 °C (relative humidity of 95 % was maintained). Mushrooms were picked when they reached a size of approximately 3.5 cm in cap diameter. The harvested mushrooms were weighed and counted per bed. Mushroom beds were watered between successive flushes (the amount of water depending on the weight of mushrooms harvested), and the mushroom cultivation was terminated after 3 flushes.

Statistical Analysis

Statgraphics® Centurion XVI version 16.1 software (Statpoint Technologies Inc., The Plains, Virginia, USA) was used to analyze the data. Analysis of Variance (ANOVA) was performed, and a p-value of <0.05 for the F-test was considered to indicate statistically significant differences between samples. Analyses were conducted in triplicate.

Results and Discussion

Synthesis and Characterization of Nanosilver Clay Composites

TEM was used to view and evaluate the distribution of AgNPs on the surfaces of the clays, and it was found that spherical NPs were evenly deposited on the surface of both zeolite (Figure 1A) and montmorillonite (Figure 1B). However, on palygorskite clay, the particles were unevenly deposited, and the concentration of these spherical AgNPs was lower when compared to those of zeolite and montmorillonite (Figure 1C). Particle size analysis revealed that AgNPs bound to zeolite clay had an average diameter of 3.33 nm, while those on montmorillonite had an average diameter of 2.85 nm (Figures A'–C').

AgNPs bound to palygorskite clay had a larger average diameter of 6.13 nm. Shameli et al.[36] obtained NPs, ranging from 2.12–3.11 nm in diameter when zeolite was used to support the synthesis of AgNPs, consistent with the average diameter obtained from zeolite in this study. Pillai et al.[28] obtained AgNPs ranging from 8–10 nm when montmorillonite was used as a support, particles much larger than the average particle sizes obtained in this study. Araujo et al.[37] found that palygorskite also yielded large AgNPs (5.5–8.94 nm), similar to those in this study. Dong et al.[38] tested the antimicrobial activity of different-sized NPs (10 nm, 30 nm, 60 nm, and 90 nm) and observed that smaller-sized AgNPs (10 nm and 30 nm sized particles) produced lower minimum inhibitory concentrations when tested against *V. natriegens.* Since NPs much smaller than that obtained by Dong et al.[38] were obtained in this study, greater antifungal activity was anticipated. Zeolite and montmorillonite had uniformly distributed, smaller AgNPs, which may be attributed to their flatter matrix structures that provided a greater surface area for AgNP adhesion.[39,40] Compared to zeolite and montmorillonite, palygorskite had fibrous rod structures, resulting in a lower surface area to bind individual AgNPs. Due to this, NPs produced from palygorskite usually occur as aggregates and clusters of large-sized NPs.[41]

The FTIR spectra of pristine zeolite and AgNP-zeolite are given in Figure 2A. The FT-IR spectrum for Zeolite showed vibration bands at 3615, 3380 cm^{-1} for O–H stretching due to the adsorbed water and at 1633 cm^{-1} for O–H bending. The band in 1021 cm^{-1} corresponds to vibration modes of asymmetric stretching of Si–O, and Al–O bonds.[42] The band at 786 cm^{-1} is assigned to stretching vibration modes of the O–Si–O and O–Al–O groups. The band found in 615 cm^{-1} is assigned to the torsional vibrations of the Al–O–Si bonds.[43] A small band at 1438 cm^{-1} is ascribed to the stretching vibration of CO_3^{2-} of calcite.[43] Although AgNP-zeolite showed similar peaks, slight alterations are observed in bands located on the 3700–3100 range cm^{-1} and regions from 1020 to 600 cm^{-1} affected by metal cations' interaction with the zeolite surface. A noticeable difference was the appearance of a peak at 1384 cm^{-1}, which indicated the existence of Ag in the composite, and this result agreed with that reported by Zhang et al.[44] The FT-IR spectra demonstrated the inflexibility of the silicate structure and the non-bond chemical interface between the silicate structure and AgNPs in the composite.[42]

The structural modification of montmorillonite after AgNP incorporation is revealed by the increase in the intensity of O–H stretching (3620 cm^{-1}), 1628 cm^{-1} (O–H bending) in plane Si–O stretching (997 cm^{-1}), Al–O stretching (914 cm^{-1})[45] associated with the aluminosilicate structure (Figure 2B). The alteration of the band intensity could be attributed to the presence of AgNPs on the defects on the octahedral sheets.[28,43] The appearance of an additional band at 1334 cm^{-1} and the downward shift in the characteristic vibrations, namely Si–O stretch (997 cm^{-1}), in comparison to the unmodified clay mineral, indicates a disturbance in the bonding in the structure of the aluminosilicate[40,44,45] and hence a more ordered structure due to the presence of AgNPs.

In the case of palygorskite (Figure 2C), the bands at 3537 and 1643 cm^{-1} were attributed to the stretching and bending vibration of surface-adsorbed water.[43] It is noteworthy that the absorption band appeared around 1330 cm^{-1} in the case of AgNP-zeolite and AgNP-montmorillonite samples was not present in AgNP-palygorskite which could be due to the relatively low loading of AgNP on the surface of the fibrous clay mineral. The general increase in the intensity of the peaks and the downward shift of Si–O stretching vibration showed some alteration in the chemical structure due to van der Waals interactions between the oxygen groups of clay minerals and AgNPs.[28] The elemental composition of the three nanosilver clay composites was studied using energy-dispersive X-ray spectroscopy (EDS). The energy peaks for Si, Al, and O, elements typically found in clays, were detected for all three clays, while peaks were obtained at 3 keV, indicating the presence of Ag on

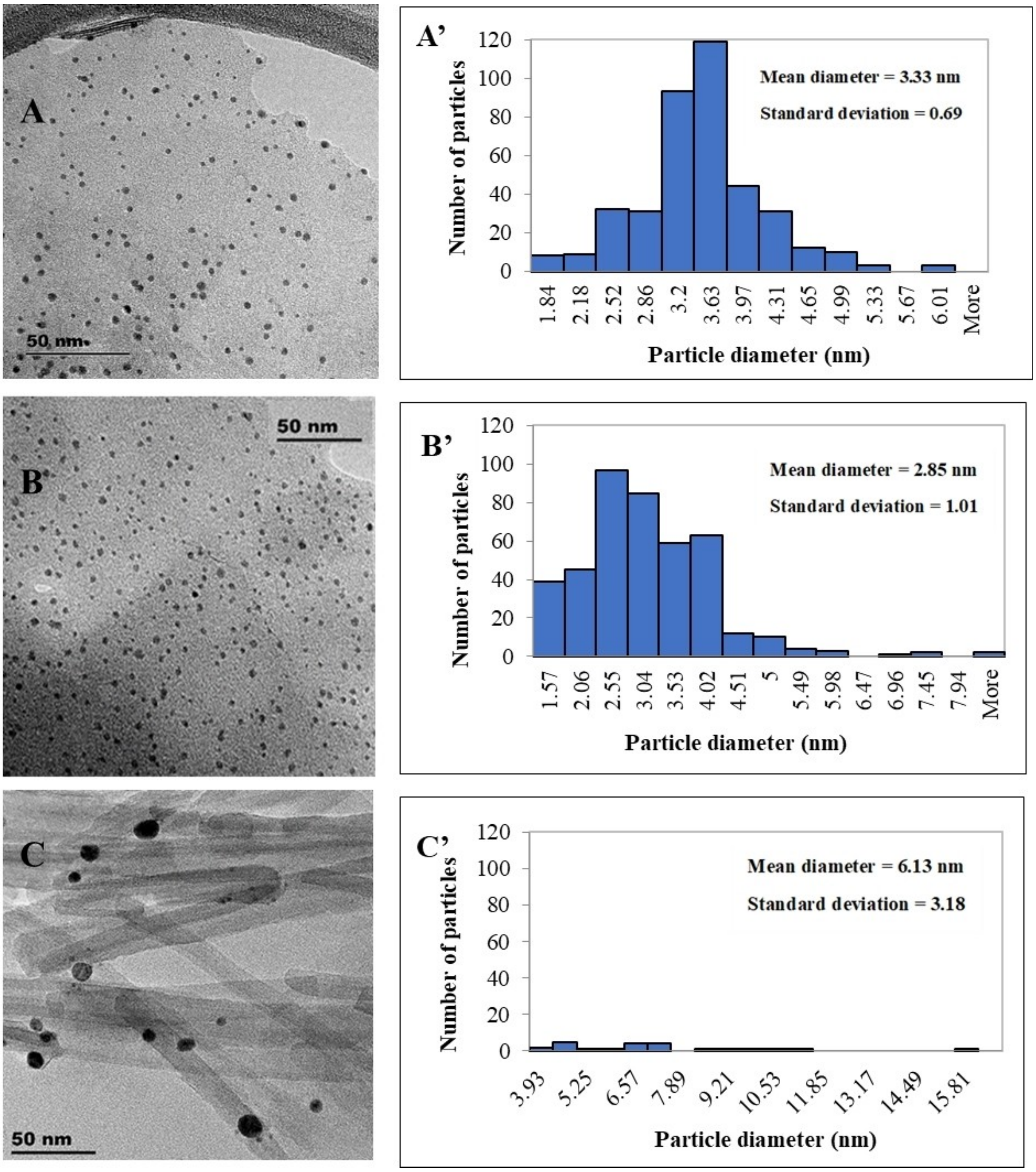

Figure 1. Transmission Electron Microscope (TEM) images (A) AgNP-zeolite; (B) AgNP-montmorillonite; (C) AgNP-palygorskite and particle size analysis data (A') AgNP-zeolite; (B') AgNP-montmorillonite; (C') AgNP-palygorskite for AgNPs bound to clays (zeolite, montmorillonite, and palygorskite):

the clays (Figures 3A to 3C). The semi-quantitative measurement of the three nanosilver clay composites (Figure 3D) showed that the average total Ag content on zeolite clay (approximately 7.03 %, which is 0.703 mg/mL of Ag) was higher than the average total Ag content on montmorillonite clay (approximately 5.86 %, which is 0.586 mg/mL of Ag). In contrast, the lowest Ag content was observed for palygorskite clay (approximately 1.41 %, or 0.141 mg/mL of Ag). There was no statistically significant difference between the Ag content on the zeolite and montmorillonite clays.

The differences in silver loading on the different clays could be attributed to the fact that surface area (especially the internal pore surface), pore size distribution, and the degree of ionization at the surface of absorbents (such as clays) influence the extent of absorption or ion carrying capacity of a matrix.[44] The low Ag content on palygorskite can be attributed to its fibrous rod-like morphology and porous channels parallel to the long axis of palygorskite crystals (where most ion exchange reactions occur).[40,44] These characteristics cause palygorskite clays to have less surface area for binding NPs and a low ion exchange capacity compared to the flatter surfaces of materials such as zeolite and montmorillonite.[46]

In addition to the size and shape of NPs, the concentration/loading of NPs on the clays greatly affects microbial toxicity.[31,47,48] In a study conducted by Pillai et al.[28] antibacterial activity was observed from a silver clay composite (tested

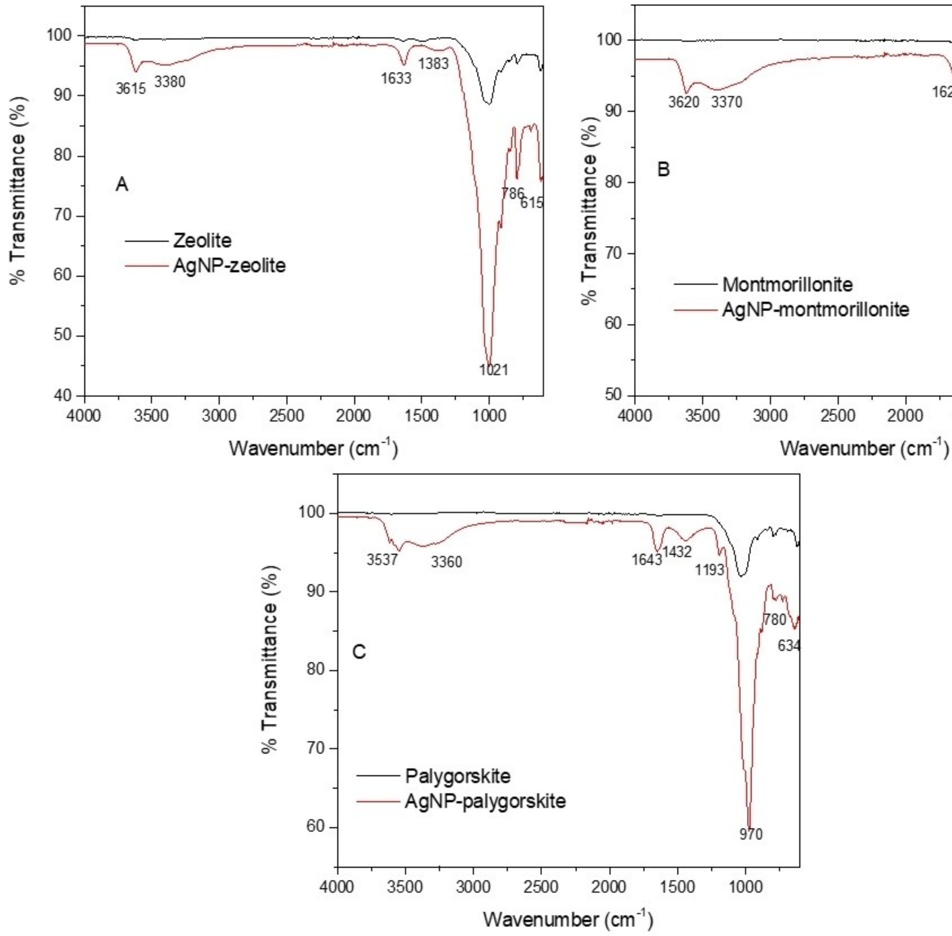

Figure 2. FTIR spectra of pristine and nanosilver clay composites (A) zeolite; AgNP-zeolite; (B) montmorillonite; AgNP-montmorillonite; (C) palygorskite; AgNP-palygorskite.

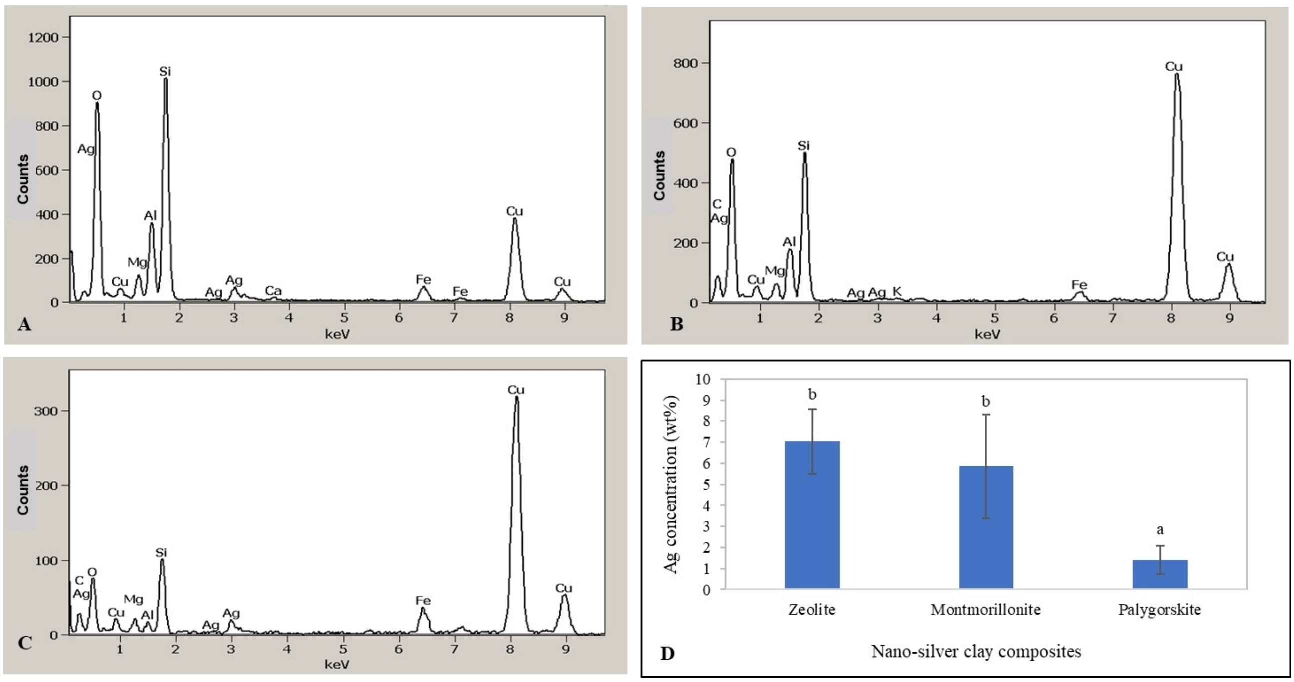

Figure 3. Energy-Dispersive X-ray Spectroscopy (EDS) spectra for nanosilver clay composites: (A) AgNP-zeolite; (B) AgNP-montmorillonite; (C) AgNP-palygorskite; (D) concentrations of Ag on montmorillonite, zeolite, and palygorskite.

against *S. aureus*, *B. cereus, E. coli*, and *P. aeruginosa*) with a silver loading of 2.3 %, much lower than the loading of Ag on zeolite and montmorillonite in this study. In addition, Missengue et al.[47] noted that the antimicrobial effect of AgNPs increases with an increase in silver loading on the support and the amount of silver that leaches from the support. Petrik et al.[49] found that Ag loading between 0.0022 mg/mL and 0.0043 mg/mL on zeolite clays was too low to demonstrate any antibacterial effect against *E. coli*. However, Shameli et al.[36] observed no superior antibacterial activity at higher Ag loadings on zeolite clay (between 0.020 mg/mL and 0.050 mg/mL) against *E. coli*, *K. pneumoniae*, and *S. aureus* and rather attributed the antimicrobial activity to smaller sized-AgNPs (between 4 nm to 8.53 nm).[50]

Effect of Nanosilver Clay Composites on the Mycelial Growth of Fungal Pathogens of *A. bisporus in vitro*.

The possibility that the clays (zeolite, montmorillonite, and palygorskite) have inherent antifungal properties was determined. The antimicrobial action of clays is attributed to the presence of reduced iron minerals, facilitating the production of reactive oxygen species, leading to the possible damage of cell membranes and intracellular proteins.[51] The fungal pathogens were inoculated on MEA-YEA, containing the three clays without AgNPs. On 2nd and 4th day, the mycelial growth of most fungal pathogens on clays was similar to the growth on the control plates (Figure 4) ($p < 0.001$). The same trend was observed on the 6th, with no inhibition of growth in the presence of the clays and, in some cases, a slight increase in mycelial growth. However, this growth increase was not significant ($p < 0.001$). It could therefore be concluded that none of the clays have any inherent antifungal activity.

The antifungal activity of the three nanosilver clay composites (AgNP-zeolite, AgNP-montmorillonite, and AgNP-palygorskite) was assessed at 1 mg/mL, 5 mg/mL, and 10 mg/mL against *A. bisporus* pathogens. The effect of the nanoclay composites on the growth of the pathogens at a concentration of 1 mg/mL is presented in Figure 5. AgNP-zeolite (1 mg/mL) caused an initial significant reduction in growth (92.9 % reduction) ($p < 0.001$) of the tested mushroom pathogens (observed on the 2nd day of cultivation). In contrast, a 78.9 % growth reduction was observed for AgNP-montmorillonite (still a significant reduction, $p < 0.001$). After four days of cultivation, the pathogens (especially the *Trichoderma* spp.) started to overcome the inhibition by the composites (inhibition reduced to 77.4 % and 58.6 % for AgNP-zeolite, and AgNP-montmorillonite, respectively). This trend continued on the 6th day of cultivation, with the inhibition of growth weakening to 51.4 % and 48.1 % for AgNP-zeolite and AgNP-montmorillonite, respectively. However, this reduction in growth was still significant ($p < 0.001$). *L. fungicola* 156 was the fungal pathogen least inhibited, with only 8.53 % and 9.90 % growth reduction on AgNP-zeolite and AgNP-montmorillonite (6th day of incubation). The pathogens showed either no growth reduction or an increase in growth in the presence of AgNP-palygorskite (throughout the cultivation period, $p > 0.05$) (Figure 5).

At a concentration of 5 mg/mL, there was a marked increase in the inhibition of the fungal pathogens, with AgNP-zeolite decreasing the average growth by 94.5 %, 96.3 %, and 94.2 % after 2nd, 4th, and 6th days of cultivation ($p < 0.001$) (7 of 9 tested pathogens were 100 % inhibited). At the same time intervals, AgNP-montmorillonite reduced the colony diameter of the

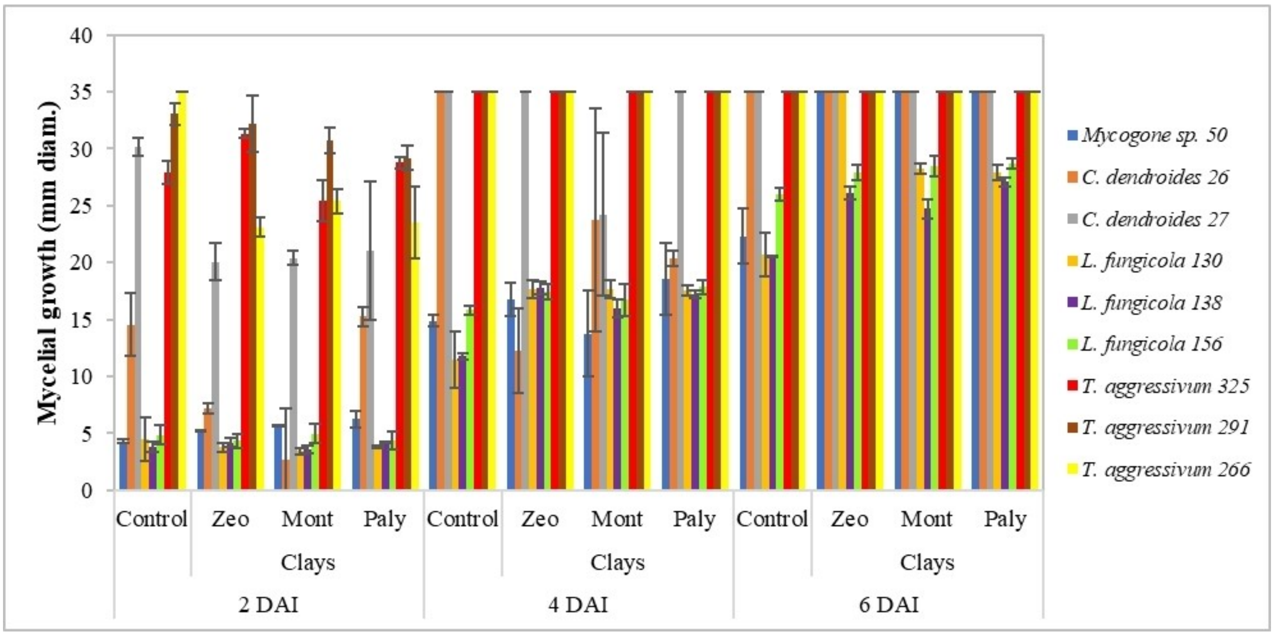

Figure 4. The effects of clays (zeolite, montmorillonite, and palygorskite) on mycelial growth of *A. bisporus* pathogens. (DAI: days after inoculation). (The *in vitro* experiments were conducted in triplicate and the data was used to derive the level of significance (critical differences at 5 % level of significance). Error bars indicate ± SD (triplicate measurements).

Research Article
doi.org/10.1002/slct.202301696

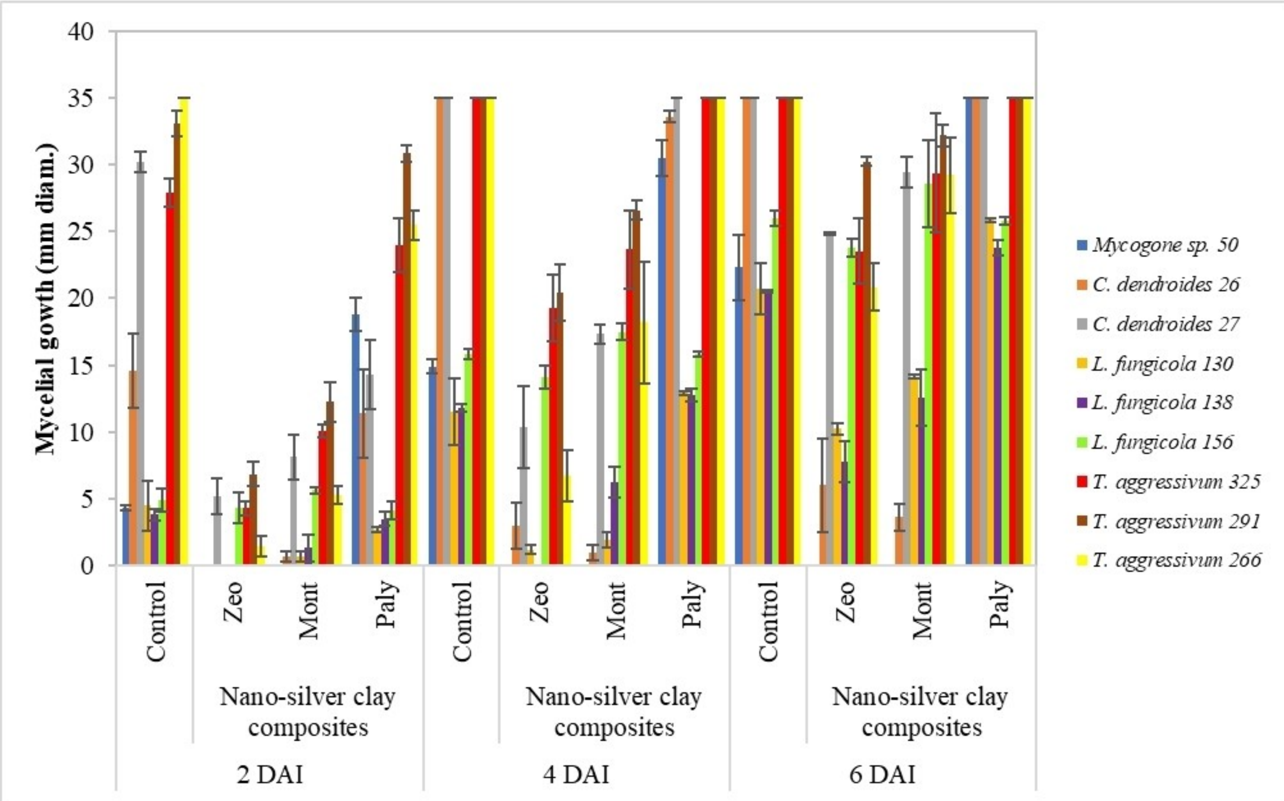

Figure 5. The effects of 1 mg/mL nanosilver clay composites (AgNP-zeolite, AgNP-montmorillonite, and AgNP-palygorskite) on the growth of *A. bisporus* pathogens. (DAI: days after inoculation). (The *in vitro* experiments were conducted in triplicate and the data was used to derive the level of significance (critical differences at 5% level of significance). Error bars indicate ± SD (triplicate measurements).

fungal pathogens by 91.3%, 91.9%, and 89.0% ($p < 0.001$) (total inhibition of 6 of the 9 tested pathogens) (Figure 6). AgNP-palygorskite failed to control the pathogens ($p > 0.05$) (*L. fungicola* growth increased), in contrast to the AgNP-zeolite and AgNP-montmorillonite, which were able to inhibit the growth of most of the mushroom pathogens tested (Figure 6).

At 10 mg/mL, AgNP-zeolite was able to inhibit 100% of the pathogens on days 2 and 4 of incubation and 99.1% of the growth of the pathogens on day 6 ($p < 0.001$) (Figure 7). AgNP-montmorillonite inhibited 99.6% of the pathogen growth on day 2 of incubation, with 99.4% and 97.7% inhibition on days 4 and 6, respectively ($p < 0.001$). AgNP-palygorskite, at 10 mg/mL, showed improved inhibition of the pathogens with a significant reduction in the growth of 70.8%, 65.04%, and 40.5% after 2, 4, and 6 days of incubation, respectively ($p < 0.001$) (Figure 7).

Two of the characteristics of nanosilver clay composites that influence their biological activity are the size and concentration of the NPs on the clay surface. This was shown very clearly in this study, where the best antifungal properties were observed for AgNP-zeolite and AgNP-montmorillonite, which had smaller average nanosilver particle sizes and higher silver loading than AgNP-palygorskite. In addition to the composite characteristics influencing the biocontrol of the pathogens, the antifungal success of nanosilver clay composites was specific to the fungal species. This was clear, for example, in the case of *T. aggressivum* where the lower concentrations of the nanosilver clay composites showed initial inhibition. Then a degree of growth recovery took place as the incubation time continued.

Furthermore, *L. fungicola* 156 showed a lower inhibition at 1 mg/mL and 5 mg/mL of the nanosilver clay composites than the other pathogens, thus affirming differences in sensitivity between species. The fungal pathogens, subjected to 5 mg/mL AgNP-zeolite, were examined using SEM for possible morphological changes due to their exposure to AgNP composites, and the results are presented in Figure 8. All pathogens showed mycelial damage and mycelial collapse (Figure 8B), while the mycelia of the fungal pathogens on the control plates (plates lacking AgNP-zeolite) appeared healthy and showed normal sporulation (Figure 8A). This phenomenon has been shown before when *S. cerevisiae* was treated with 4 mg/mL AgNPs and *C. albicans* with 0.5 to 2 mg/mL AgNPs and structural damage to the membranes, formation of pits causing leakages of internal cell components, and eventual cell death were observed.[52–54] Ouda[53] also found shrinkage and collapse of the hyphae when *A. alternata* and *B. cinerea* were grown on agar plates containing 15 mg/mL AgNP. From the above, it is apparent that, depending on the treatment concentrations, structural changes in the hyphae, cell wall deformations, membrane damage, and alterations in spore formation and germination will result from AgNP exposure.

The findings in this study are not unique, as it is apparent throughout the literature that sensitivity to AgNPs varies

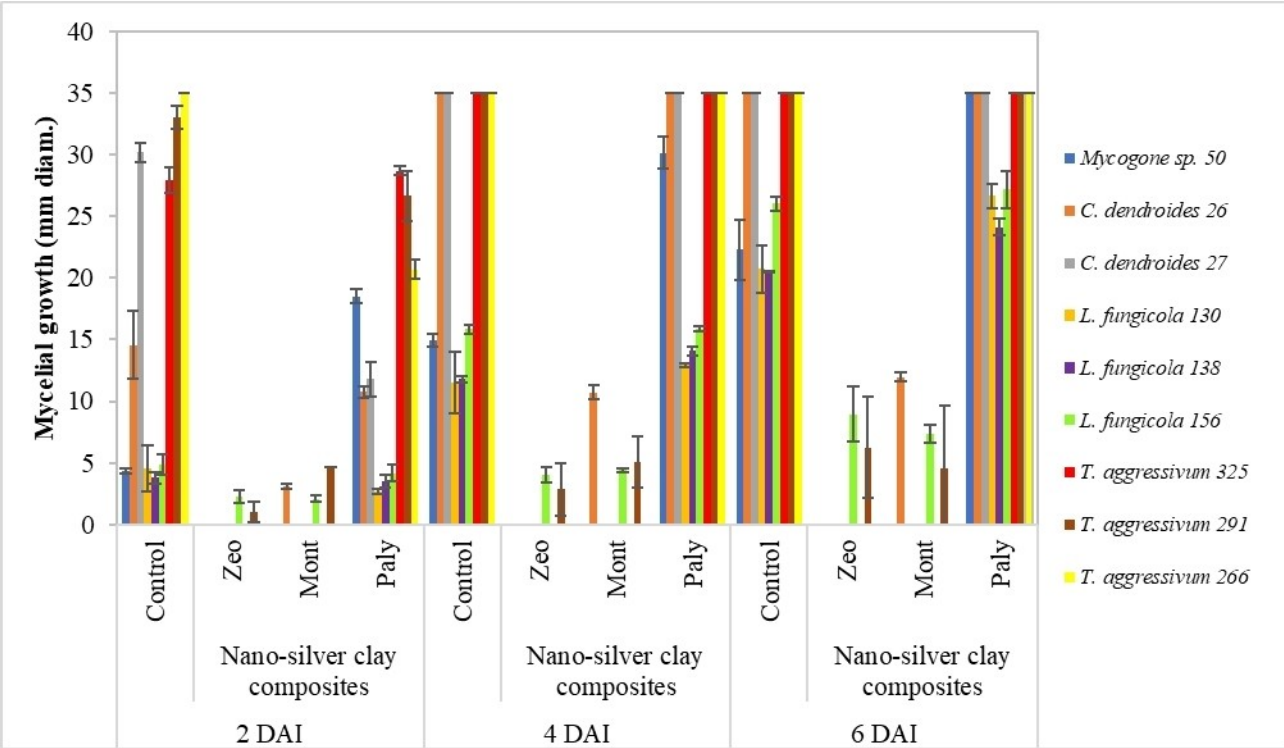

Figure 6. The effects of 5 mg/mL nanosilver clay composites (AgNP-zeolite, AgNP-montmorillonite, and AgNP-palygorskite) on the growth of *A. bisporus* pathogens. (DAI: days after inoculation). (The *in vitro* experiments were conducted in triplicate, and the data was used to derive the level of significance (critical differences at 5% level of significance). Error bars indicate ± SD (triplicate measurements)

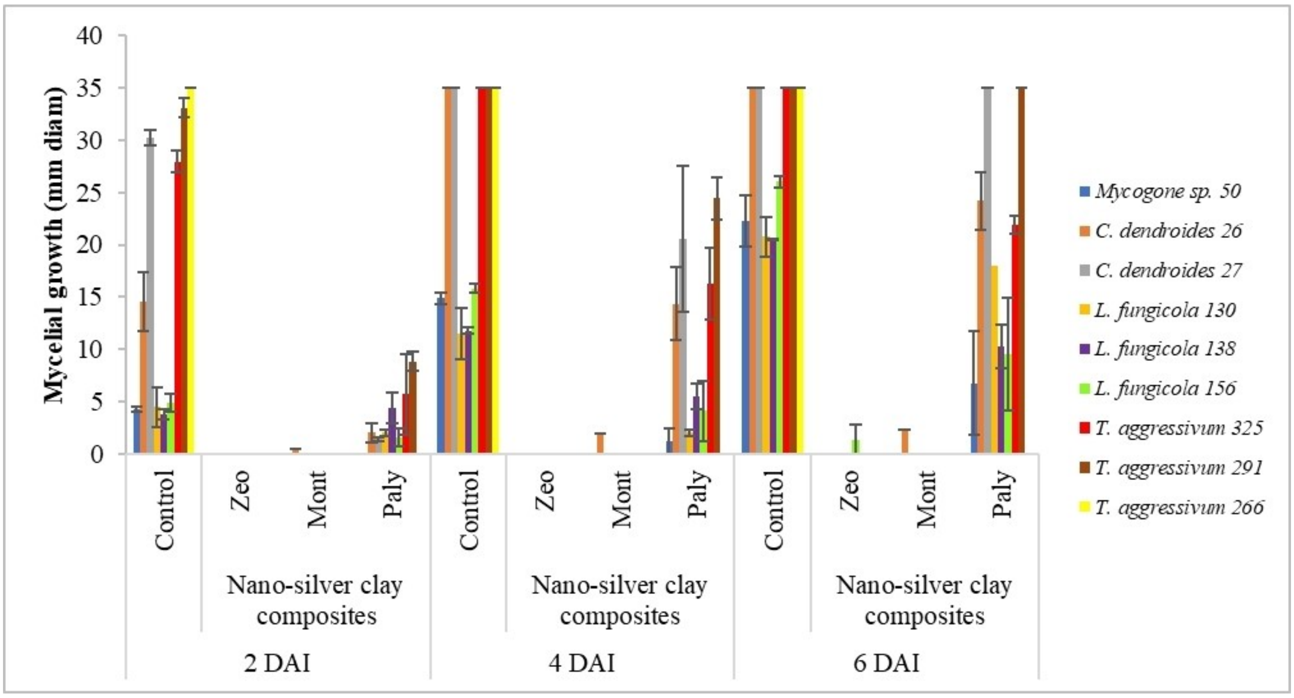

Figure 7. The effects of 10 mg/mL nanosilver clay composites (AgNP-zeolite, AgNP-montmorillonite, and AgNP-palygorskite) on the growth of *A. bisporus* pathogens. (DAI: days after inoculation). (The *in vitro* experiments were conducted in triplicate, and the data was used to derive the level of significance (critical differences at 5% level of significance). Error bars indicate ± SD (triplicate measurements).

between fungal species. It has been shown that the growth of *A. flavus* and *F. solani*, pathogens of cocoa crops, were not significantly affected by 0.1 mg/mL AgNPs.[55] In contrast, the antifungal properties of AgNPs have been demonstrated

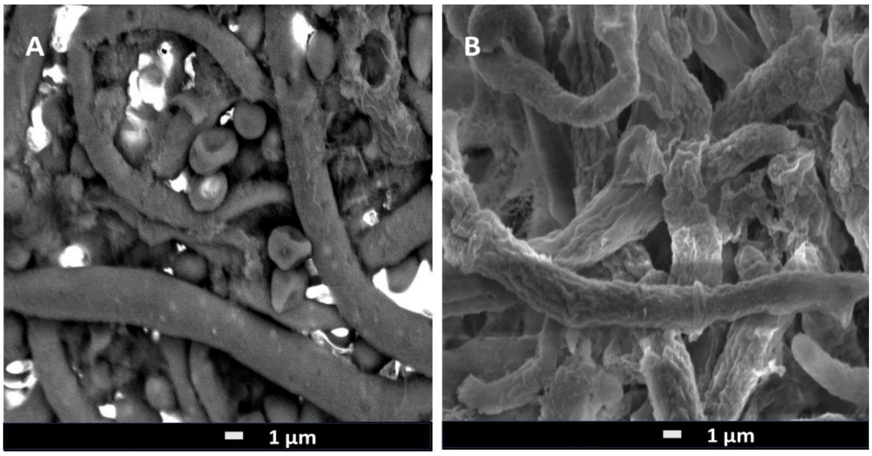

Figure 8. Scanning Electron Microscopic images of *T. aggressivum* f. *aggressivum* 266, following growth on plates containing (A) no AgNP-zeolite healthy mycelia and spores and (B) 5 mg/mL of AgNP-zeolite showing the mycelial collapse.

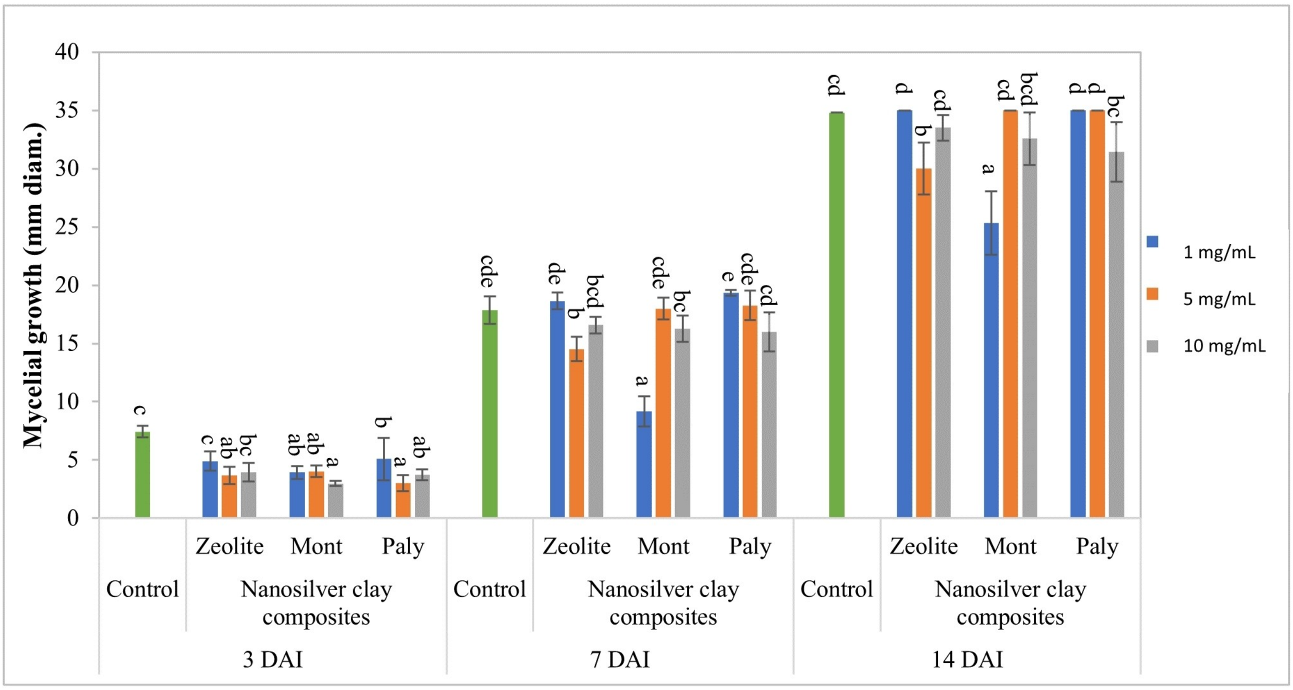

Figure 9. Effect of different AgNP-clay composites on mycelial growth of *A. bisporus* (Mean values with the same letter/s in the same cluster are not significantly different ($p > 0.05$)). (DAI: days after inoculation) (The *in vitro* experiments were conducted in triplicate and the data was used to derive the level of significance (critical differences at 5% level of significance). Error bars indicate ± SD (triplicate measurements).

against *B. sorokiniana*, *Colletotrichum* spp., *C. albicans*, and *S. cerevisiae*.[56] Significant inhibition of certain *Colletotrichum* spp. has also been observed[20] when this fungus was exposed to between 0.03 and 0.1 mg/mL AgNPs,[56] while exposing *F. oxysporum* to 1 mg/mL AgNPs reduced mycelial growth by only 24% and at a concentration of 5 mg/mL it inhibited colony sizes by 65%.[57] It should be noted that in this study, the AgNPs were in a composite form with a clay matrix. The AgNP-zeolite concentration that gave the maximum inhibition (i.e., 10 mg/mL), contained a silver concentration of 0.7 mg/mL, in the range of silver concentrations that showed antifungal activity in the above-cited literature. In a study on the release of silver ions and their mechanisms of antibacterial action, Nagy et al.[58] observed that AgNP-zeolite gradually released Ag ions into the media (i.e., Luria Bertani broth), resulting in bacterial death. It is assumed that the antimicrobial activity of the nanosilver clay composites was due to the enhanced absorption of the AgNP-clay complexes, which resulted in the better intracellular release of Ag ions.[59] It is possible that the effective interaction of the fungal surface with AgNPs, immobilized on clay surfaces, could be the significant factor contributing to the success of the clay nanocomposites in controlling the mushroom pathogens in this study.

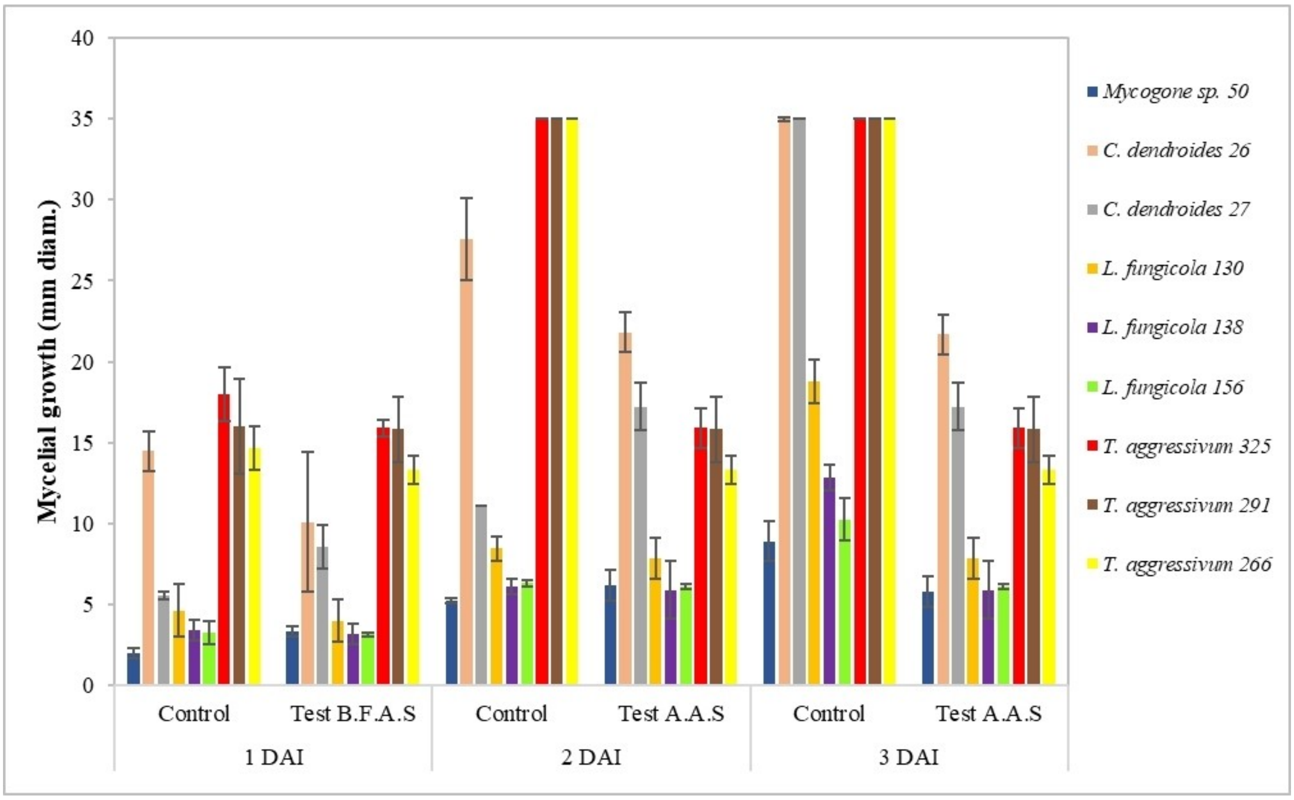

Figure 10. The effect of 10 mg/mL AgNP-zeolite solution on actively growing *A. bisporus* pathogens. (B.A.S: Before Addition of AgNP-zeolite solution; A.A.S: After Addition of AgNP-zeolite solution) (DAI: days after inoculation). (The *in vitro* experiments were conducted in triplicate and the data was used to derive the level of significance (critical differences at 5% level of significance). Error bars indicate ± SD (triplicate measurements).

Effect of Nanosilver Clay Composites on the Mycelial Growth of *A. bisporus in vitro*

As the nanosilver clay composites effectively controlled the mycopathogens, the effect of these clay composites on the growth of *A. bisporus* (at the same concentrations) was determined (Figure 9). There was very little to no inhibition of *A. bisporus* growth when cultivated on the optimized extract growth medium containing nanosilver clay composites (AgNP-zeolite, AgNP-montmorillonite, and AgNP-palygorskite) at 1 mg/mL, 5 mg/mL and 10 mg/mL when compared with mycelial growth from control plates (extract medium with no nanosilver clay composites).

A reduction in mycelial growth was observed from AgNP-montmorillonite at 1 mg/mL and AgNP-zeolite at 5 mg/mL on the 14^{nth} day, approximately 13.9% and 27.13% lower than the growth of the control, respectively (Figure 9). Except for these, the difference in mycelial growth on any of the nanosilver clay composites (at all concentrations) and the control were statistically non-significant. On the 14th day, the growth of *A. bisporus* at 10 mg/mL of AgNP-zeolite, AgNP-montmorillonite, and AgNP-palygorskite was reduced by only 3.76%, 6.43%, and 9.68% (respectively) compared to the control. Therefore, the nanosilver clay composites had a negligible effect on the mycelial growth of *A. bisporus*. This was important because, at this concentration, AgNP-zeolite and AgNP-montmorillonite fully inhibited most fungal pathogens.

The results of this study show that the nanosilver clay composites are not indiscriminate and selectively inhibit the fungal pathogens, while not affecting the host fungus (*A. bisporus*), an observation that has also been shown in other studies where toxic trace elements, including silver, did not have any adverse effect on *A. bisporus*, either the mycelial growth or the production of fruiting bodies.[60] It was found that *A. bisporus* is highly selective in its accumulation of elements, a possible explanation for its insensitivity when growing in the presence of silver. In addition, *A. bisporus* is used to conduct extracellular synthesis of AgNPs, implying the presence of silver ion-reducing enzymes that could infer resistance to this metal.[55] However, further studies are required to confirm this. Other studies have shown control of cobweb disease by AgNPs without affecting *A. bisporus*.[61] According to a recent article,[62] extracellular enzymes present in the mushroom can act as a stabilizing agent and help reduce the toxicity of AgNPs. Furthermore, it was demonstrated that the supernatant of bacteria from the mushroom-casing environment *B. velezensis*, selectively inhibited the growth of *T. aggressivum*.[63,64] The proteomic analysis of the response of *T. aggressivum* and *A. bisporus* after exposure to *B. velezensis* supernatant showed an increased abundance of stress response proteins in *T. aggressivum* with a concurrent decrease in growth proteins and antioxidants. In contrast, exposure of *A. bisporus* to *B. velezensis* supernatant showed no effect on the growth of *A. bisporus* and no stress-induced proteins were evident. It can be speculated

Research Article
doi.org/10.1002/slct.202301696

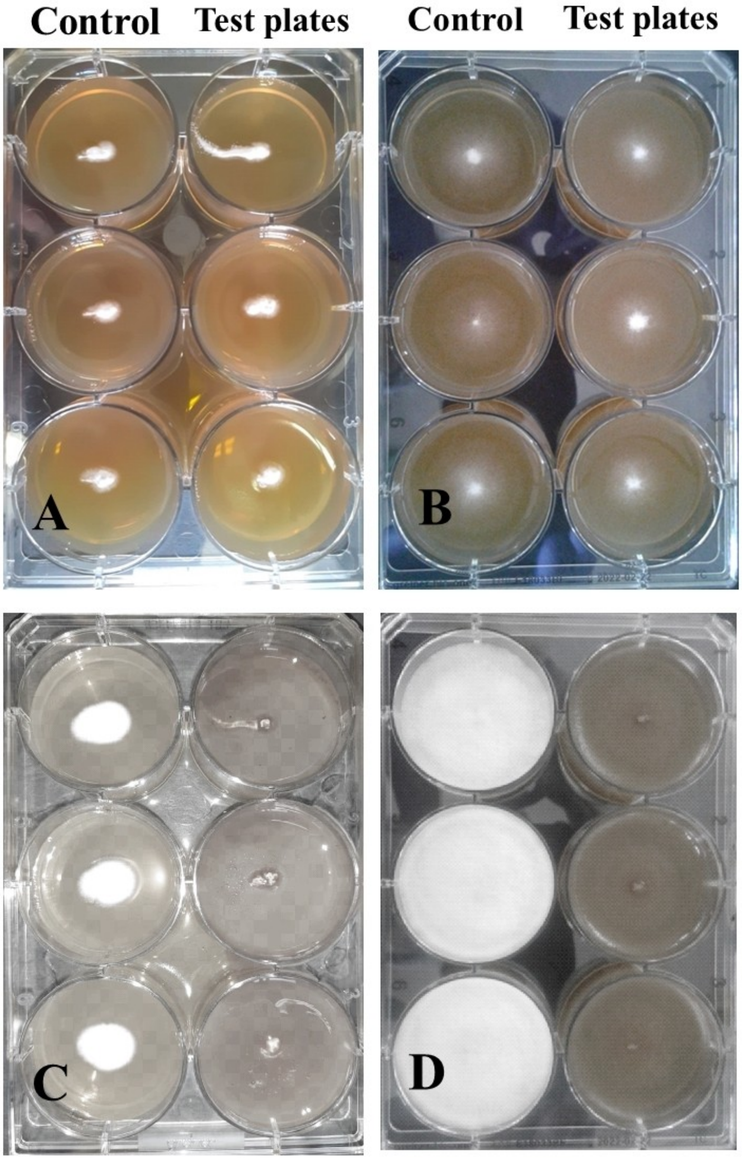

Figure 11. Growth of fungal pathogens before and after the addition of 10 mg/mL AgNP-zeolite solution: (A) *L. fungicola* 130 before the addition (2 days of incubation); (B) *T. viride* 102 before the addition (1 day of incubation); (C) left row (control) – *L. fungicola* 130 on plate with no AgNP-zeolite: right row (test plate)- mycelia exposed to AgNP-zeolite (4 days after addition of solution); (D) left row (control) – *T. viride* 102 on plate without AgNP-zeolite: right row (test plate) – mycelia exposed to AgNP-zeolite (2 days after addition of solution).

that similar differences in the interaction of AgNPs (from the clay mineral composites) with the fungal pathogens in the presence of *A. bisporus* exist. A detailed investigation is, however, required to unravel the mechanism of selective antifungal activity observed in this study.

Effect of AgNP-Zeolite Solution Actively Growing Fungal Pathogens *in vitro.*

Of the three tested nanosilver clay composites, 10 mg/mL AgNP-zeolite was the most effective in inhibiting the growth of the various fungal mycopathogens. Its inclusion into the growth medium of the pathogens (in vitro study) suggests that it can serve as a disease-preventative agent, should it be added to the growth material used in mushroom beds. However, whether the AgNP-zeolite could be used curatively on actively growing mushroom fungal pathogens as a spray solution was unknown. To determine this, the fungal pathogens were allowed to grow for 2 days in the case of the *Mycogone* sp., *C. dendroides*, and *L. fungicola*, while for *T. aggressivum*, only 1 day of growth was allowed (due to its fast growth rate), before the addition of the AgNP-zeolite solution. Before adding AgNP-zeolite, the colony sizes of the actively growing pathogens on the control and test plates were similar ($p > 0.05$). After adding the AgNP-zeolite solution, the mycelial growth on the test plates for all the fungal pathogens stopped, and the colony sizes and development remained unchanged from the time of spray application

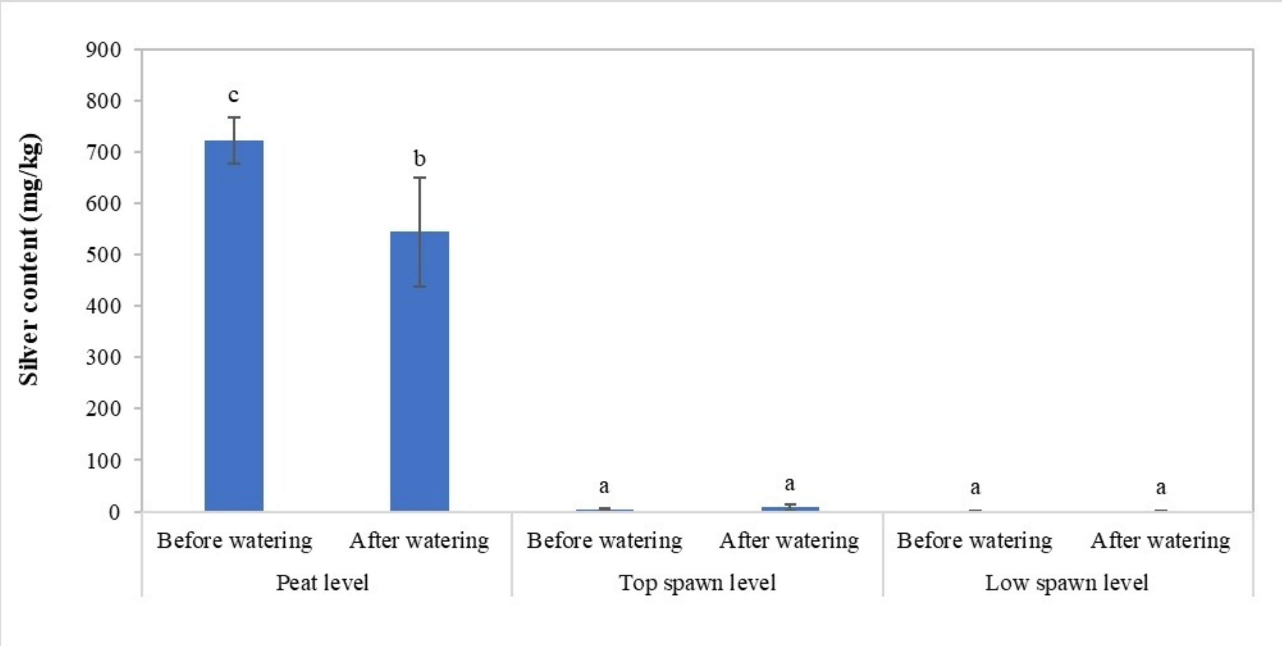

Figure 12. Silver content determined by ICP-OES from different mushroom bed levels, following extensive watering (Mean values with the same letter/s in the same cluster are not significantly different ($p > 0.05$)). (The *in vivo* experiments were conducted in replicates of five and the data was used to derive the level of significance (critical differences at 5% level of significance). Error bars indicate ± SD (triplicate measurements).

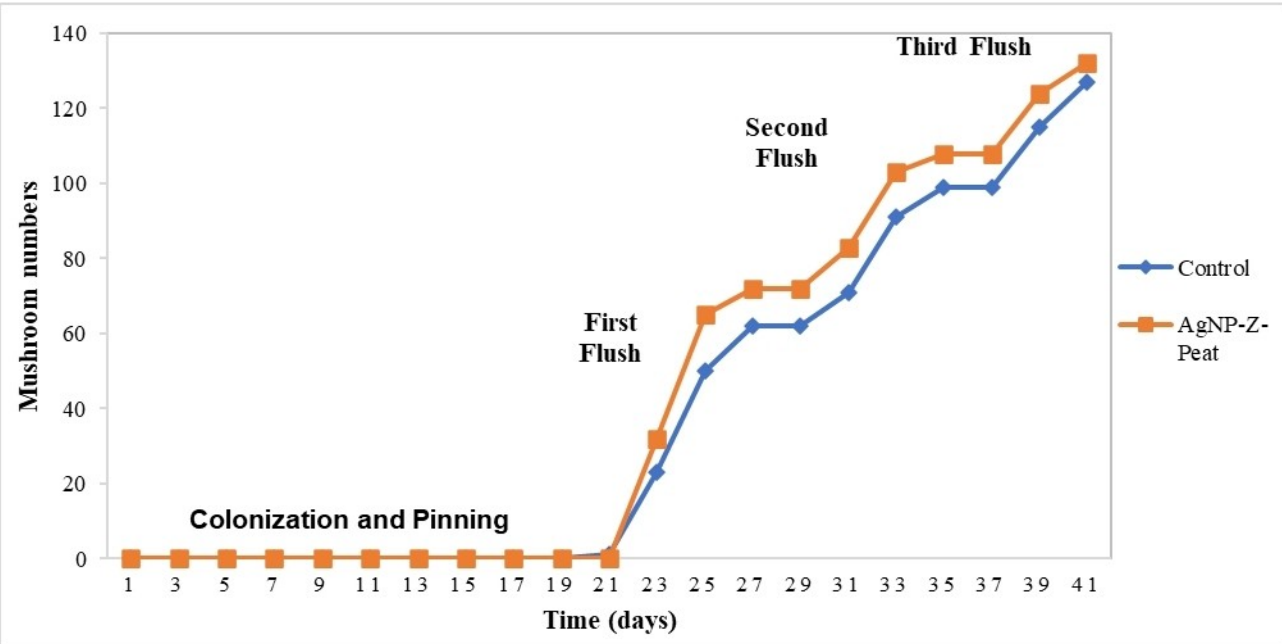

Figure 13. Number of mushrooms produced by *A. bisporus*, cultivated in the presence and absence of 10 mg/mL AgNP-zeolite applied to peat.

throughout the incubation period (Figure 10). The lack of growth and development of the fungi after application of the AgNP-zeolite solution is shown in Figure 11 for *L. fungicola* and *T. viride*.

This showed that AgNP-zeolite, at 10 mg/mL, can stop further growth and development of mushroom fungal pathogens when applied as a spray on the actively growing pathogens. The curative treatment/inhibition of the fungal pathogens is advantageous as it will reduce the application cost drastically compared to the application of the AgNP-zeolite to the mushroom beds. In addition, the difficulty of safely discarding the mushroom substrate (containing AgNPs), to minimize its environmental impact, will be alleviated.

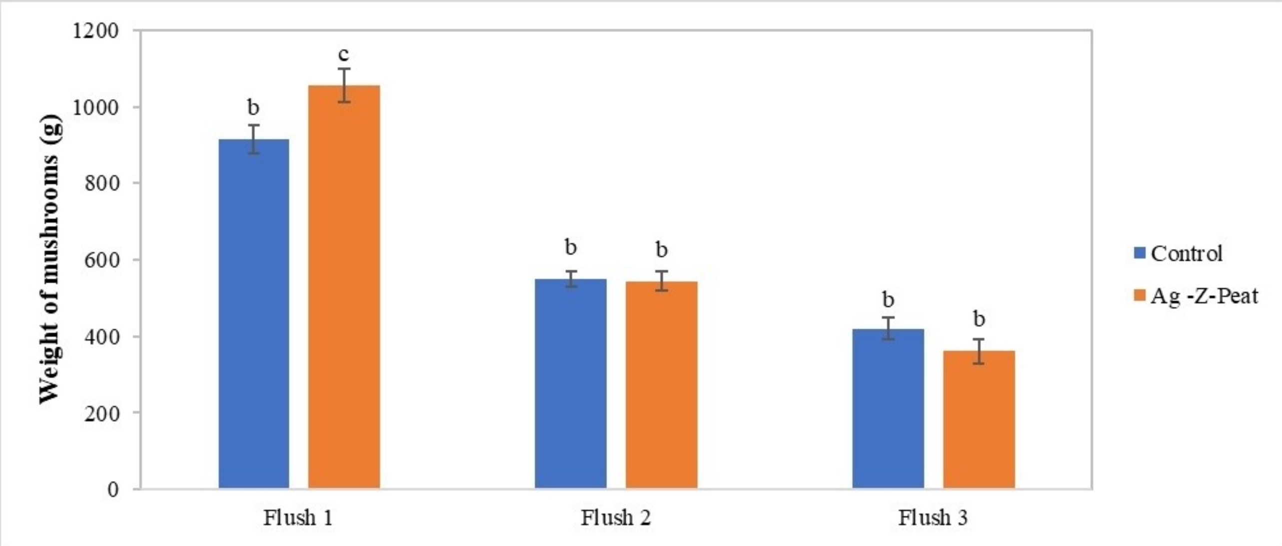

Figure 14. Total weight of mushrooms produced by *A. bisporus*, cultivated in the presence and absence of 10 mg/mL AgNP-zeolite, mixed into the peat. Mean values with the same letter/s in the cluster are not significantly different ($p > 0.05$). (The *in vivo* experiments were conducted in replicates of five and the data was used to derive the level of significance (critical differences at 5 % level of significance). Error bars indicate ± SD (triplicate measurements).

Effect of AgNP-Zeolite on the Growth and Mushroom Production by *A. bisporus in vivo.*

Any pesticide used to prevent fungal pathogens in mushroom cultivation would need to be added to the casing material, as this is where most of the severe mushroom diseases develop. Therefore, 10 mg/mL AgNP-zeolite was incorporated into the casing material. There was a possibility that the AgNP-zeolite may leach out and be lost from the mushroom beds (thus nullifying its potential effects) during the extensive watering required in early mushroom cultivation (i.e., in the first 5 days following casing). The possible leaching of AgNP (due to watering) was determined at 3 levels of the cultivation beds by measuring the silver concentrations using ICP-OES. After the watering period, there was still a high average concentration of Ag (544 mg/kg) in the peat layer when compared to the average Ag concentration (722 mg/kg) before the watering (Figure 12). Although a decrease is apparent (a 25 % loss of Ag), 75 % of the Ag was retained in the peat layer. The average Ag concentration in the top spawn level was low (4.31 mg/kg) before watering. It increased slightly (8.32 mg/kg) after watering (Figure 12). At the same time, the average Ag concentration in the lower spawn mix level was low throughout the watering period (approximately 0.87 mg/kg and 0.45 mg/kg before and after watering). The Ag content before and after watering for both the top and lower spawn layers was statistically insignificant (Figure 12).

For the successful cultivation of mushrooms, extensive watering is required for the first 5 days after applying the casing to the compost (compost with water content below 65 %).[65] Although watering led to a loss of some AgNPs, the concentration of Ag that remained is still high enough to control most fungal pathogens.

For the first 3 days of cultivation, there were very little to no visible mycelial growth on any control (5 beds) or AgNP-zeolite peat (AgNP-Z-Peat) beds (5 beds). From the 6th to 19 days of cultivation, the surface of the control beds became extensively colonized and covered by mushroom mycelia. At the same time, there was little to no mycelial growth visible on the surfaces of AgNP-Z-Peat beds. By the 9th day of cultivation, pinhead formation was on the control beds, while on the AgNP-Z-Peat beds, very few pinheads were observed. All beds, however, started producing mushrooms of suitable size from the 21st day, with control beds showing slightly higher numbers than the AgNP-Z-Peat beds initially (Figure 13). However, from the 23rd day until the end of cultivation, AgNP-Z-Peat beds showed mushroom production similar to the control beds (Figure 13).

Most mushrooms (on all beds) were produced during the first flush, decreasing gradually in subsequent flushes, with the lowest numbers observed in the third flush (Figure 13). During the first flush, AgNP-Z-Peat beds produced 16 % more mushrooms than the control beds. In the second flush AgNP-Z-Peat beds produced slightly lower mushroom numbers than in control beds (2 % fewer mushrooms). During the last flush, AgNP-Z-Peat beds produced only 4 % fewer mushrooms than the control beds (Figure 13). However, considering all three flushes, AgNP-Z-Peat beds produced similar numbers of mushrooms to the control beds (approximately 3.9 % more mushrooms were produced on AgNP-Z-peat beds).

The combined weight of mushrooms obtained corresponded to the numbers obtained from the control and test beds (Figure 14). AgNPs do not significantly affect mushroom numbers or mushroom weight. The highest combined mushroom weight was observed on the first flush and gradually decreased in the subsequent flushes (Figure 14). Cultivation beds containing AgNP-Z-Peat had the highest combined mushroom weight during the first flush (approximately 1056.09 g), with the control beds producing slightly less (approximately 914.68 g). During the second flush, the control beds produced mushroom weights similar to that of the AgNP-Z-Peat beds, while the third flush produced by the control beds yielded mushrooms with a slightly higher combined weight (approximately 420.67 g) than AgNP-Z-Peat beds (approximately 360.78 g) (Figure 14). The overall mushroom weight (over the three flushes) was slightly higher in AgNP-Z-Peat beds than in the control beds. These results were surprising since initially, AgNP-Z-Peat beds produced no visible mycelia and pinheads on the bed surfaces, and it was therefore anticipated that fewer mushrooms would result. However, the AgNP-zeolite did not affect mushroom fruiting.

There are reports in the literature that some fungicides, known to control fungal pathogens of mushrooms, have a negative effect on the development of mushroom mycelia and yield. Prochloraz-Mn (the only registered fungicide for use in South Africa's mushroom industry) has been known to cause a notable yield loss during mushroom production due to damage to the *A. bisporus* mycelial cell walls.[14] Fungicides such as benomyl, thiophanate methyl, iprodione, and mancozeb have also been shown[14] to significantly inhibit the growth of *A. bisporus* at 25 mg/L and higher concentrations. The antifungal activity of AgNP-zeolite (particularly at 10 mg/mL) against mushroom pathogens (preventative and curative) has been demonstrated in this study (in vitro) and AgNP-zeolite, when applied to the peat of mushroom beds (preliminary *in vivo* study), had no adverse effects on mushroom fruiting yields, thus showing promise as a fungicide for use in the mushroom industry.

Conclusions

Management of fungal diseases of food crops like mushrooms is challenging and, at the same time, economically important. This study evaluated silver clay nanocomposites as a fungicide material for mushroom pathogens, focusing on overcoming synthetic fungicide flaws. Findings from the current investigation demonstrated that different clay surfaces (zeolite, montmorillonite, and palygorskite) functionalized with AgNPs were very effective against mushroom phytopathogenic fungi. These clay surfaces functioned as support matrices to AgNPs and allowed excellent particle size control, minimizing NPs' agglomeration during synthesis. The small dispersion of AgNPs on clay surfaces greatly influences the overall antifungal activity, with small-sized NPs more efficient in controlling the pathogenic fungi. NPs bound to montmorillonite and zeolite were smaller and more evenly distributed than those bound to palygorskite (fibrous clay). It was shown in this study that all three nanosilver clay composites (added preventatively) exerted antifungal activity against the selected fungal pathogens that affect *A. bisporus* (*C. dendroides, L. fungicola, T. aggressivum* f. *aggressivum* and *Mycogone* sp). There was a direct correlation between the level of inhibition of the fungal pathogens and the increase in the concentration of the nanosilver clay composites. None of the nanosilver clay composites tested was found to have a severe adverse effect on *A. bisporus* growth at any of the concentrations tested, despite effectively inhibiting the growth of the mushroom fungal pathogens. These findings are vital because the ideal fungicide should be species-specific, controlling target organisms with little to no effect on the host organism. When AgNP-zeolite (10 mg/mL) was applied curatively to actively growing fungal pathogens, no further growth or spore development was observed for any of the pathogens. The *in vivo* study showed that including AgNP-zeolite in mushroom, beds did not influence *A. bisporus* mycelial growth or fruiting. This study affirmed the antifungal properties of AgNPs and the potential use of nanosilver clay composites as alternative fungicides against mushroom pathogens without adversely affecting mushroom production. The curative action of AgNP-zeolite used as a solution demonstrated that these particles could be limited to affected areas in the mushroom beds, reducing the cost of application and the possible toxic effects of AgNPs. This will also limit the environmental impact of silver contamination when discarding the cultivation material. A work clearly shows the prospects of the silver clay nanocomposites in mushroom cultivation; however, data on the material's efficacy on the commercial-level application are needed to establish whether this alternative control method is viable in a real-time agricultural setting. Furthermore, the mechanism of selective action of the nanocomposites toward the mushroom pathogens needs to be investigated in detail.

Acknowledgements

The authors thank the Department of Biotechnology and Food Technology at the Tshwane University of Technology, National Research Foundation (NRF), and the Centre for Nanostructures and Advanced Materials, Council for Scientific and Industrial Research (Project No. C1E0080), Department of Science and Innovation (Project No. C6E0046), South Africa, for the financial support.

Conflict of Interests

The authors declare no conflict of interest.

Data Availability Statement

The data that support the findings of this study are available from the corresponding author upon reasonable request.

Keywords: Nanosilver clay composites · *A. bisporus* · mushroom pathogens · antifungal properties

[1] F. J. Gea, M. J. Navarro, M. Santos, F. Diánez, J. Carrasco, *Microorganisms* **2021**, *9*, 585–609.
[2] N. C. Snelders, G. C. Petti, G. C. M. van den Berg, M. F. Seidl, B. P. H. J. Thomma, *bioRxiv*. **2021**, 47847–47884.

[3] J. Avalos, M. C. Limón, *Encyclopedia* **2022**, *2*, 1–13. https://doi.org/10.3390/encyclopedia2010001.
[4] R. Xu, X. Liu, B. Peng, P. Liu, Z. Li, Y. Dai, S. Xiao, *Pathogenesis* **2020**, *9*, 232–248.
[5] S. Kamal, A. Barh, K. Sharma, V. P. Sharma, *in Agricultural Biotechnology: Latest Research and Trends* (Eds.: D. K. Srivastava, A. K. Thakur, P. Kumar), Springer, Singapore, **2021**, pp.661–688.
[6] D. Li, F. L. Sossah, Y. Yang, Z. Liu, Y. Dai, B. Song, Y. Fu, Y. Li, *Pathogenesis* **2019**, *8*, 179–192.
[7] J. Clarke, H. Grogan, D. Fitzpatrick, K. Kavanagh, *Eur. J. Plant Pathol.* **2022**, *163*, 369–379.
[8] F. Memarzadeh, B. Sharifnabi, R. Eslamizadeh, *Fungal Biol.* **2020**, *7*, 259–261.
[9] H. Allaga, A. Zhumakayev, R. Büchner, S. Kocsubé, A. Szucs, C. Vágvölgyi, L. Kredics, L. Hatvani, *Agronomy* **2021**, *11*, 2434–2448.
[10] D. Kosanovic, H. Grogan, K. Kavanagh, *Fungal Biol.* **2020**, *124*, 814–820.
[11] A. A. Hassan, M. T. Ibrahim, *IOP Conf. Ser. Earth Environ. Sci.* **2022**, *1060*, 072021–072037.
[12] D. G. Medvediev, A. O. Kerner, S. V. Bondaruk, G. A. Al-Maali, *Ukr. Bot. J.* **2019**, *76*, 121–131.
[13] A. Chakwiya, E. J. Van der Linde, L. Chidamba, L. Korsten, *Eur. J. Plant Pathol.* **2019**, *154*, 767–776.
[14] S. Altaf, S. K. Jan, S. A. Ahanger, U. Basu, R. A. Rather, O. A. Wani, F. Rasool, M. Mushtaq, M. T. Yassin, A. A. F. Mostafa, *J. Fungi.* **2022**, *8*, 554–576.
[15] J. Carrasco, G. M. Preston, *Environ. Microbiol.* **2020**, *22*, 858–872.
[16] F. J. Gea, M. J. Navarro, M. Santos, F. Diánez, D. Herraiz-Peñalver, *Agronomy* **2019**, *9*, 656.
[17] D. Shokouhi, A. Seifi, *Biocatal. Agric. Biotechnol.* **2020**, *30*, 101848–101854.
[18] K. M. Thambugala, D. A. Daranagama, A. J. L. Phillips, S. D. Kannangara, I. Promputtha, *Front. Cell. Infect. Microbiol.* **2020**, *10*, 604923–604942.
[19] G. M. Preston, J. Carrasco, F. J. Gea, M. J. Navarro, *Biological Control of Microbial Pathogens in Edible Mushrooms.* (Eds B. Singh, B. Lallawmsanga, A. Passari, (eds). Springer, Cham. **2018**.
[20] F. J. Gea, M. J. Navarro, M. Santos, F. Diánez, D. Herraiz-Peñalver, *Agronomy.* **2019**, *9*, 656–680.
[21] M. A. Aslani, B. Harighi, J. Abdollahzadeh, *BioControl* **2018**, *119*, 20–26.
[22] J. Carrasco, G. M. Preston, *Environ. Microbiol.* **2020**, *22*, 858–872.
[23] Z. K. Taha, S. N. Howar, G. M. Sulaiman, *Res. J. Pharm. Tech.* **2019**, *12*, 1320–1326.
[24] D. R. Ibraheem, N. N. Hussein, G. M. Sulaiman, H. A. Mohammed, R. A. Khan, O. Al Rugaie, *Nanomaterials* **2022**, *12*, 2808–2833.
[25] D. G. Hirpara, H. P. Gajera, D. D. Savaliya, R. V. Bhadani, *J. Microbiol.* **2021**, *59*, 1031–1043.
[26] R. V. Bhadani, H. P. Gajera, D. G. Hirpara, D. D. Savaliya, S. A. Anuj, *Arch. Microbiol.* **2022**, *204*, 311–326.
[27] S. Mansoor, I. Zahoor, T. Baba, S. Padder, Z. Bhat, A. Koul, L. Jiang, *Front. Nanotechnol.* **2021**, *3*, 679358–679370.
[28] S. K. Pillai, S. S. Ray, M. Scriba, J. Bandyopadhyay, M. P. Roux-Van Der Merwe, J. Badenhorst, *Appl. Clay Sci.* **2013**, *83*, 315–321.
[29] T. Bruna, F. Maldonado-Bravo, P. Jara, N. Caro, *Int. J. Mol. Sci.* **2021**, *22*, 7202–7223.
[30] H. P. Gajera, D. G. Hirpara, R. V. Bhadani, B. A. Golakiya, *BioMetals* **2022**, *35*, 479–497.
[31] I. Akpinar, U. Muammer, T. Sar, *SN Appl. Sci.* **2021**, *3*, 506–515.
[32] W. Badar, M. A. Ullah-Khan, *IET Nanobiotechnol.* **2020**, *14*, 331–340.
[33] N. Hojnik, M. Modic, Y. Ni, G. Filipic, U. Cvelbar, J. L. Walsh, *Environ. Sci. Technol.* **2019**, *53*, 1893–1904.
[34] A. Gibała, P. Żeliszewska, T. Gosiewski, A. Krawczyk, D. Duraczyńska, J. Szaleniec, M. Szaleniec, M. Oćwieja, *Biomol. Eng.* **2021**, *11*, 1481–1451.
[35] M. A. Hayat, *Principles and techniques of Electron Microscopy. Biological Applications.* 4th ed. Cambridge University Press. **2000**.
[36] K. Shameli, M. B. Ahmad, M. Zargar, W. M. W. Yunus, N. A. Ibrahim, *Int. J. Nanomed.* **2011**, *6*, 331–341.
[37] C. M. Araújo, S. M. das Virgens, C. A. do Nascimento Cavalcante, L. C. Nunes, L. C. Bertolino, C. A. de Sousa-Brito, H. M. Barreto, C. E. Eiras, *Mater. Sci. Eng. C* **2020**, *115*, 1110927.
[38] Y. Dong, H. Zhu, Y. Shen, W. Zhang, L. Zhang, *PLoS One* **2019**, *14*, e0222322.
[39] E. Matras, A. Gorczyca, S. W. Przemieniecki, M. Oćwieja, *Sci. Rep.* **2022**, *12*, 18046.
[40] C. M. Araújo, C. E. Eiras, M. das Virgens-Santana, A. do Nascimento-Cavalcante, *Revista Geintec-Gestao Inovacao E Tecnologias* **2020**, *10*, 5456–5470.
[41] S. I. Hossain, E. A. Kukushkina, M. Izzi, M. C. Sportelli, R. A. Picca, N. Ditaranto, N. Cioffi, *Nanomaterials.* **2023**, *13*, 848.
[42] S. A. Abdel-Gawad, A. M. Fekry, *Sci. Rep.* **2022**, *12*, 9136.
[43] N. N. Safie, A. Zahrim Yaser, N. Hilal, *Asia Pacific Chem. Eng. J.* **2020**, *15*, 2448–2457.
[44] H. Zhang, F. Yang, Q. Zhang, A. Hui, A. Wang, *ACS Appl. Bio. Mater.* **2022**, *5*, 3960–3971.
[45] M. Diana-Carme, R. Dumitra, G. Ana-Maria, R. Ana-Maria, C. V. Andrei, Z. Valentin, N. Ileana-Denisa, *Molecules.* **2022**, *2*, 5791–5810.
[46] .M. R. Abukhadra, S. M. Ibrahim, S. M. Yakout, M. E. El-Zaidy, A. A. Abdeltawab, *Energy Convers. Manage.* **2019**, *196*, 739–750.
[47] R. N. M. Missengue, N. M. G. Musyoka, Madzivire, O. Babajide, O. O. Fatoba, M. Tuffin, F. L. Petrik, *J. Environ. Sci. Health Part A.* **2016**, *51*, 97–104.
[48] Q. Zhang, H. Zhang, A. Hui, Y. Lu, A. Wang, *Results Mater.* **2023**, *18*, 100396–100406.
[49] L. Petrik, R. Missengue, O. Fatoba, M. Tuffin, J. Sachs, WRC Report KV297/12. Gezina, South Africa, **2012**.
[50] E. Selem, A. F. Mekky, W. A. Hassanein, F. M. Reda, Y. A. Selim, *Saudi J. Biol. Sci.* **2022**, *29*, 103457–103463.
[51] P. E. Dim, L. S. Mustapha, M. Termtanun, J. O. Okafor, *Arab. J. Chem.* **2021**, *14*,103064–103078.
[52] Q. He, Q. Chen, R. Zhu, S. He, G. Lv, C. Gu, A. Wang, *Clays Clay Miner.* **2022**, *70*, 809–823.
[53] M. Ouda, *J. Microbiol.* **2014**, *9*, 34–42.
[54] L. Yang, Q. Zhang, Q. Wang, W. Ding, K. Zhang, *Membranes* **2021**, *11*, 889–906.
[55] R. Villamizar-Gallardo, J. F. O. Cruz, O. O. Ortíz-Rodrigues, *Presq. Agropec. Bras.* **2016**, *51*, 1929–1936.
[56] K. Lamsal, S. W. Kim, J. H. Jung, Y. S. Kim, K. S. Kim, Y. S. Lee, *Microbiology* **2011**, *39*, 194–199.
[57] J. Abkhoo, N. Panjehkeh, *Int. J. Infect. Dis.* **2017**, *4*, 41126–41129.
[58] A. Nagy, A. Harrison, S. Sabbani, R. S. Munson, P. K. Dutta, J. W. Waldman, *Int. J. Nanomed.* **2011**, *6*, 1833–1852.
[59] J. Szaleniec, A. Gibała, J. Stalińska, M. Oćwieja, P. Żeliszewska, J. Drukała, M. Szaleniec, T. Gosiewski, *bioRxiv.* **2022**, doi: https://doi.org/10.1101/2022.01.03.474872.
[60] S. Budzyńska, M. Silwulski, A. Budka, P. Kalač, P. Niedzielski, M. Gąsecka, M. Mleczek, *J. Fungi.* **2022**, *8*, 883–900.
[61] I. Potočnik, E. Rekanović, M. Stepnović, S. Milijašević-Marčić, B. Todorović, L. Nikolić-Bujanović, M. Čekerevac, *Pesticidi I fitomedicina.* **2014**, *29*, 283–289.
[62] A. M. Al-Dbass, S. A. Daihan, A. A. Al-Nasser, L. S. Al-Suhaibani, J. Almusallam, B. I. Alnwisser, S. Saloum, R. S. Alotaibi, L. A. Alessa, R. S. Bhat, *Molecules* **2022**, *27*, 7656–7666.
[63] D. Kosanovic, M. Dyas, H. Grogan, K. Kavanagh, *Euro. J. Plant Pathology.* **2021**, *160*, 397–409.
[64] D. G. Hirpara, H. P. Gajera, *Appl. Organometal Chem.* **2020**, *34*,54075422.
[65] M. J. Navarro, J. Carrasco, F. J. Gea, *Agronomy.* **2021**, *11*, 2063–2075.

Manuscript received: May 16, 2023